

# Highlight and Specular reflection removal in photogrammetric techniques applied to Architectural Heritage 3D modeling

<sup>1</sup>Fabrizio Ivan Apollonio  
fabrizio.apollonio@unibo.it  
<sup>1</sup>Andrea Ballabeni  
andrea.ballabeni@unibo.it  
<sup>1</sup>Marco Gaiani  
marco.gaiani@unibo.it

<sup>1</sup>Department of Architecture,  
Università di Bologna

## ABSTRACT

In this paper, we present a new technique to remove specular effects from the photogrammetric results in a automatic photogrammetric workflow for Architectural Heritage (AH) 3D model construction. Our solution provides a new reconstruction pipeline completely integrated in the automatic photogrammetric pipeline re-using existing data to arrange new results. The process of acquisition of the images to get the finished 3D model is therefore unique and the process for acquiring and visualizing the correct perceived color is fully integrated with the process of shape capture. Overall, the method does not require specific technical knowledge, being therefore relatively easy to use, and it can be used over many different urban settings and contexts. The proposed methodology is a high-level image-processing algorithm. As such, it uses several lower-level methods for its building blocks. We consider these methods as black boxes, and we explain below their input, output and purpose.

We demonstrated the efficiency of our method using case study of our work in many cases of the ca 43 km of historical porticoes system in Bologna, Italy, a superset of the family of AH objects that it belongs to.

## KEYWORDS

3D modelling, Structure from Motion, Automatic photogrammetry, Specular removal, Image processing, Color mapping, Reflection component separation

**Received** 18 February 2016; **Revised** 01 June 2017; **Accepted** 02 June 2017

**CITATION:** Apollonio F. I., Ballabeni A., Gaiani M. (2017) 'Specular reflection removal in the context of SFM techniques for Architectural Heritage 3D models construction', *Cultura e Scienza del Colore - Color Culture and Science Journal*, 07, pp. 39-57, DOI: 10.23738/ccsj.i72017.04

---

**Fabrizio Ivan Apollonio**, Full Professor at University of Bologna, Dept. of Architecture, and PhD in Survey of the existing Built Heritage (University of Ancona). His main research topics lies on Virtual reconstruction, semantic modeling and application in the field of ICT to Cultural Heritage and development of information/cognitive systems aimed to fruition, study and documentation of CH.

**Andrea Ballabeni**, neuroscientist at heart and computer scientist for trade, he has worked for the largest Italian software companies as software developer and project manager during the last decade. He has a PhD in neuroscience and a master degree in Experimental psychology. He is now research technician and Senior software developer at Department of Architecture – University of Bologna.

**Marco Gaiani** is Full Professor of Architectural Representation at the University of Bologna and past Director of Director of the Design Dept. of the Politecnico of Milano and DAPT of University of Bologna. A specialist in 3D computer imaging, modelling and visualization for Heritage and archaeology, he was one the first developers/user of laser scanning technology in the Cultural Heritage field and also developed photogrammetry-related technologies.

## 1. INTRODUCTION

In the field of Architectural Heritage (AH), 3D model construction and visualization, using techniques based on photogrammetric techniques, is increasingly becoming a key approach, ensuring ease of use and efficient results, even for non-professional [1]. Significant progress has been recently achieved in the areas of efficient algorithms for scalable image matching [2], large-scale bundle adjustment [3], and in generating dense and well-calibrated clouds of point as output [4], the core components of the photogrammetric pipeline. As a result, it is nowadays possible to easily reconstruct large scenes from image sequences and at low cost [5].

The topic of AH 3D reconstruction and architectural modeling from images, in particular, has received considerable attention in the last decade [6], and also our research group developed in this area an efficient pipeline based on automatic photogrammetry to integrate accurate shape and color capture, reproduction and visualization using web-based real-time rendering techniques in [7].

An unsolved issue of our pipeline concerns the problems arising from specular reflections effects. The appearance of specular reflections is inevitable in AH urban environment, due to the characteristics of materials existing in real world. These effects typically appear in areas with polished floors (i.e. marble), or in presence of windows or shop windows, determining scattering effects in geometry and incorrect values of diffuse reflectance.

Specular reflection are critical flaws, affecting image quality and, then, the final results of each photogrammetric pipeline. Specifically, dense point clouds generation and faithful color reproduction are task having difficulties if specular reflections exist in the input images. E.g. acquired textures with the presence of highlights produce distinct loses of details. These problems are generally a side effect of the generally shared assumption by computational approaches that scene surfaces are composed of pure diffuse reflection. However, for a wide variety of inhomogeneous materials in real world, the reflection includes both diffuse and specular components. Hence, algorithms that are usually based on an ideal Lambertian can completely fail when facing the specular reflection. So far, specular removal methods need to be used in order to improve the photoconsistency based image-to-surface registration as well as for 3D model reconstruction of surfaces with specular reflection component.

Diffuse and specular reflections are produced by different physical interactions between light and object surfaces. According to the neutral

interface reflection model [8], the color of the specular reflection is identical to that of the illumination, while the color of the diffuse reflection is the intrinsic characteristic of the object. With these assumptions, specular removal can be viewed as the general problem of extracting information contained in an image and transforming it into certain meaningful representation. This representation is able to describe the intrinsic properties of the input image, and it is well known under the name of intrinsic images introduced by [9].

Several characteristics of the original input image can be defined as intrinsic images: illumination color and geometry, surface reflectance and geometry and view-point [10]. In our case, the two intrinsic characteristics that must be extracted are the diffuse and the specular reflection components. We reuse the diffuse reflection and we discard the specular one.

In this paper, we present a new technique to remove specular effects from the photogrammetric results. Our solution provides a new reconstruction pipeline completely integrated in the automatic photogrammetric pipeline reusing existing data to arrange new results. The process of acquisition of the images to get the finished 3D model is therefore unique and the process for acquiring and visualizing the correct perceived color is fully integrated with the process of shape capture. Overall, the method does not require specific technical knowledge, being therefore relatively easy to use, and it can be used over many different urban settings and contexts. Our processing is semi-automatic and use the photographs employed in the 3D textured model construction using a standard photogrammetric pipeline.

From a functional point of view is part of the image pre-processing phase. Image pre-processing methods are fundamental to improve the image quality for successful photogrammetric processing. Indeed, being the image processing fully automated, the quality of the input images, in terms of radiometric quality as well as network geometry, is fundamental for a successful 3D reconstruction. In detail our solution exploits two existing steps - (a) image color balance and exposure compensation, and (b) image denoising - introducing a new extra-step (c) image highlight removal. This last is the key step of the pipeline and represents the main novelty.

To enable this last new processing, the central idea is the use of SIFT Flow algorithm, a technique based on dense optical flow research started more than 30 years ago with the work of Horn and Schunck [11]. We refer to publications like [12, 13, 14] for a detailed overview of optical flow methods and the general principles behind it.



Figure 1 - Typical problems of the automatic photogrammetry pipeline in presence of specular effects

SIFT Flow technique align two images sharing similar scene characteristics by matching SIFT descriptors instead of raw pixels. SIFT Flow allows matching densely sampled SIFT features between two images, while preserving spatial discontinuities [15], to align the images such that a pixel-wise comparison can be made across the input set. Gradients with variation across the image set are assumed to belong to the reflected scenes while constant gradients are assumed to belong to the desired

background scene. By correctly labeling gradients belonging to reflection or background, the background scene can be separated from the reflection interference. Unlike previous approaches that exploit motion, our approach does not make any assumptions regarding the background or reflected scenes geometry, nor requires the reflection to be static. Our specular removal technique is based on [16], but further customizations were introduced and finally the technique was integrated in our automatic

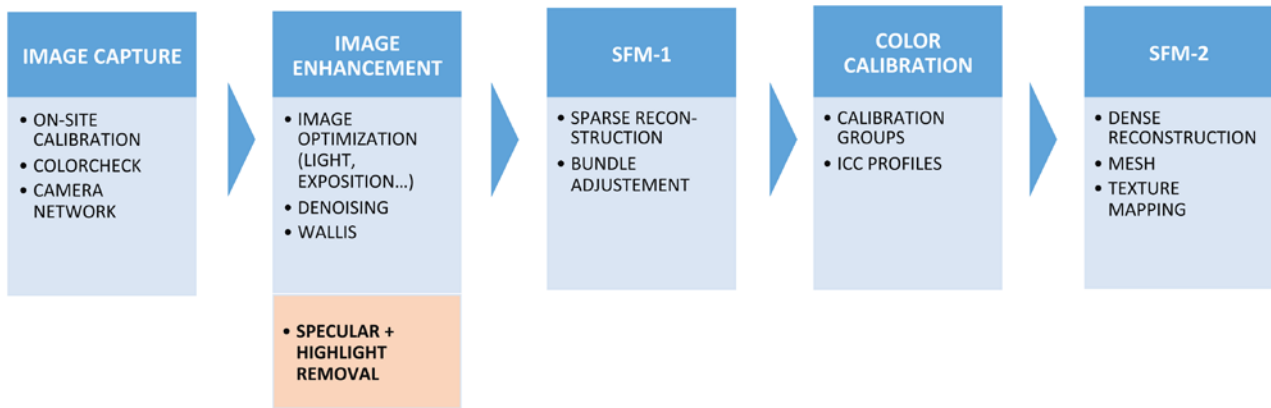


Figure 2 - Our automatic photogrammetry pipeline with the specular removal phase on orange background.

photogrammetric pipeline (Figure 2). We tested our method using as case study example from a building with arcades in Bologna, a superset of our field of interest because it presents all the problems to which we want give solution.

## 2. PROBLEM CHARACTERIZATION & RELATED WORKS

Figure 3 shows images taken under the porch of a building. In these images, we can see two of the most typical and frequent problems that appear in real-world 3D shape and color capture of urban systems related to specular reflections problems:

- Polished pavements presenting highlights caused by different light sources;
- A scene image behind a glass pane. This is the case of 'shop window', where one takes a photograph of an object behind a window. The glass will produce an unwanted layer of reflection in the final image. The reflection from the glass interferes with the view of the interior of the shop behind the shield.

In the determination of the diffuse reflection surfaces, traditionally these two phenomena are treated as different problems, one known as specular removal and the second as layers separation. In this paper, we present a technique that aims to model the two phenomena as two sides of the same coin. In our approach, specular and diffuse reflections are assimilated to different layers. In this way, the two problems are brought back to the solution of a single problem known as separation layers, where the captured image  $I$  is a linear combination of a reflection layer  $I_R$  and the desired background scene,  $I_B$ , as follows:

$$I = I_R + I_B \quad (1)$$

The goal of reflection removal is to separate  $I_B$  and  $I_R$  from an input image  $I$  as shown in Figure 10. Three reasons led to this choice:

- The approach allows the development of a solution completely integrated in the existing pipeline, easy to implement, and completely automatic;
- The histogram of the tonal distribution of images with specular effects (see Figure 4) does not show the typical behavior of images with highlights where data appears on the right side. For this reason, the results obtained through image processing techniques, or acquiring High Dynamic Range (HDR) images, in the elimination of specular reflections, are unsatisfactory;
- Recently, a great effort of Computer Vision community was devoted to the progress of efficient techniques of layer separation. Separating illuminant and re-reflection is a well-known problem as demonstrated by Marc Ebner works [17]. Several solutions well fit the boundaries of our problems and establish a solid ground on which to develop a specific appropriate solution.

In [18] is presented a complete survey of specular removal techniques, with a useful classification to select a proper method for a specific application. The survey classifies methods for separating reflection components into two categories by the number of images used: Multi-image or Single-image methods. The first category uses multiple images taken under specific conditions (e.g. view-point, lighting direction, etc.) and benefits from the fact that for varying viewing directions, the diffuse and specular reflections behave differently. The techniques are based on histogram methods [19], high-low frequency separation [20], multi-baseline-stereo [21], deriving intrinsic images from image sequences with illumination changes [22], color and polarization methods [23] and multi-flash methods [24]. All these

approaches can be further categorized as Local or Global depending on how the information is used.

Highlight removal using a single image is generally much more challenging. The single-image approaches are based on using color reflection model [25], 2D diagram approach [26], use of specular-free image [27], Partial Differential Equation (PDE) approach [28], use of color information and classifier [29], separation of highlight reflections on textured surfaces [30], Fresnel methods [31]. In the single-image category, there can be further two categories aiming to identify and separate diffuse color pixels: Neighborhood analysis, Color Space analysis.

In case of first category, neighborhood pixels are examined to infer the diffuse information usually by propagating from outside the highlight towards the inside. However, discontinuities in surface colors can make difficult for diffuse information to be accurately transferred [30]. The second category is based on color distributions to distinguish between diffuse and specular components. However, many factors such as image noise or color blending at edges can cause cluttering in color space, which can impair such approaches.

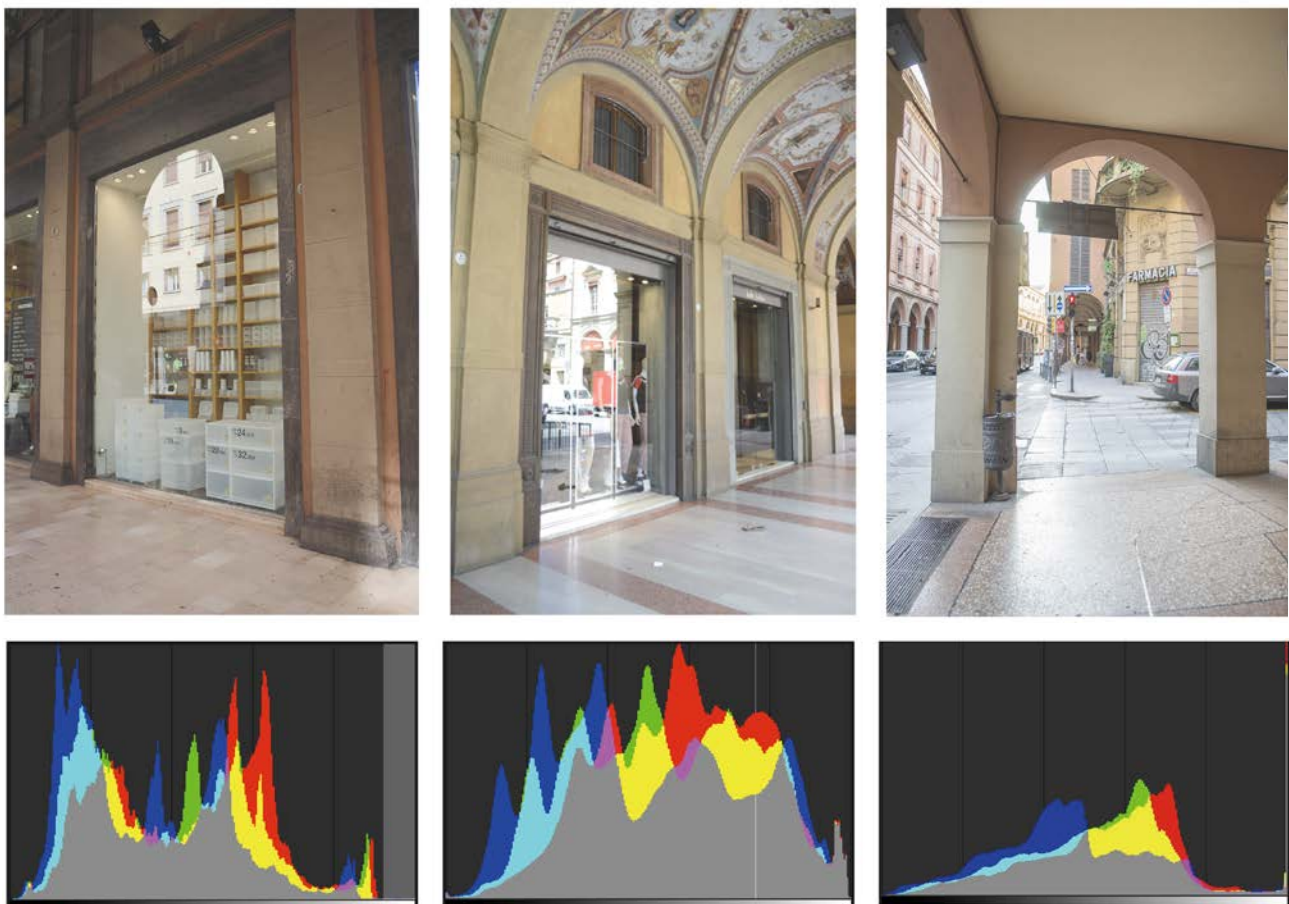
As mentioned earlier, the problem is highly ill-posed, therefore these approaches are not free from limitations. For example, in [25] color clustering is very sensitive to noise. Polarization

methods like [23] are, at the moment, very promising tools also in our field of application [32], but this paper would like to present a different technique. Polarimetric techniques, in effect, require a rotating polarization filter in front of the main capture camera. However, this aspect of capture can be automated, even on a single camera, and excellent data quality. The method proposed in [30] uses color segmentation and polarization filter to remove specular effect retaining geometrical information but the color value is shifted. The method in [23] uses pixel level dichromatic reflection model, however, both this and [31] needs an estimation of illuminant source.

Following [18] consideration and experimentation results, and a series of tests carried out by us to verify the suitability of specific algorithms to our cases, we could state that although the currently available methods achieve good component separation results, they are limited by the conditions of their applicability. In particular, most of the techniques rely on a specific reflection model and assume that the specular reflectance varies insignificantly with wavelength, which means that its color is essentially that of the light source. This assumption, together with their sensitivity to the noise, reduces the range of applications where these methods can be used. Furthermore, most part of these algorithms presents strong light requirement. Unfortunately, we are in the case

Figure 3 - Typical reflection problems in the urban context: shop windows and specular reflections on the floor.

Figure 4 - Figure 3 images histogram.



of uncontrolled light, with materials existing in real world, as well as areas with polished floors (i.e. marble), or in presence of windows or shop windows, that limits a lot the number of solution available.

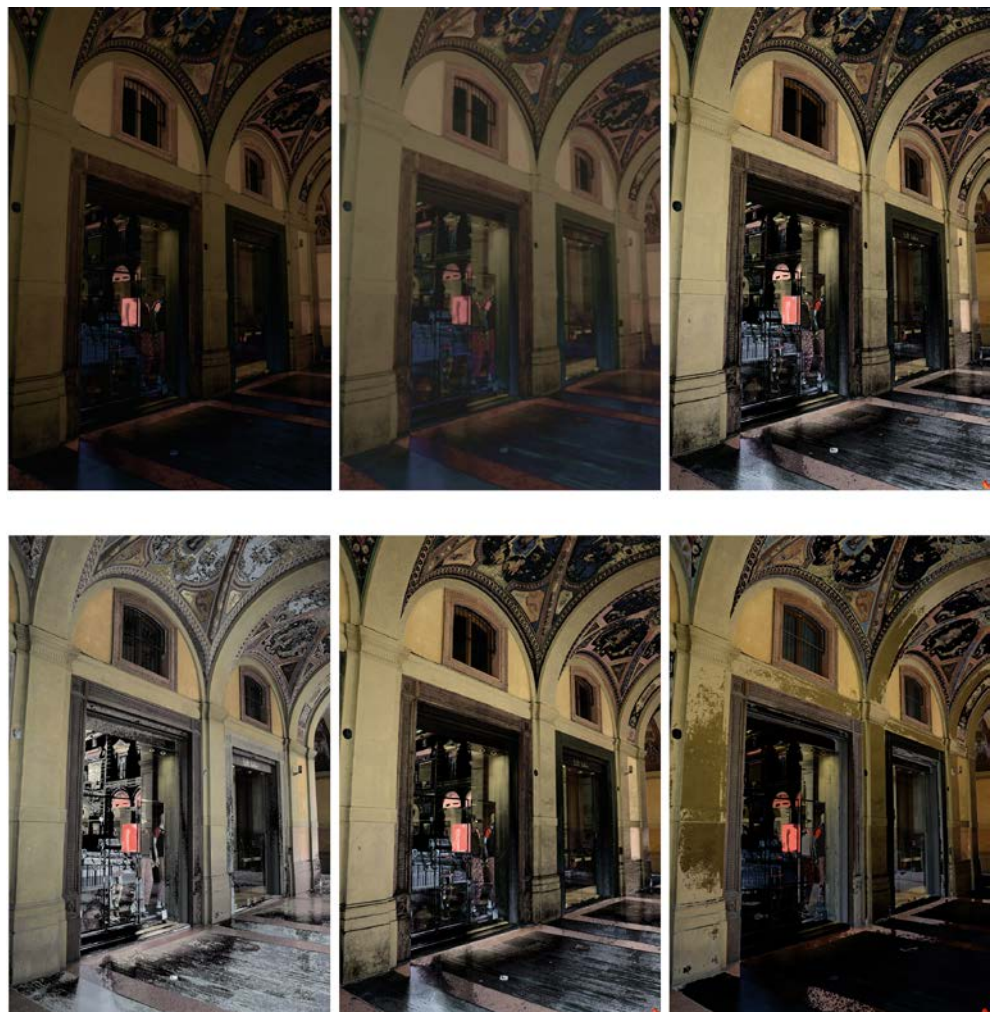
Finally, the number of effects that these algorithms are able to manage are limited compared to the complexity of the interactions in the real world. Mainly, specular regions are generally composed of a core part and extended specular region. The core part has lost information while extended region has partial image information. Most of the work available in literature address the removal of a single specular region, however, the removal of both regions individually retaining maximum possible information is not properly discussed especially for large specular regions.

This last problem appears to be crucial in our case. Effective solutions to mitigate it are essentially based on manual segmentation, a long, tedious and an easily error-prone process. From the point of view of the algorithm we focused, initially, on single images techniques, based on Shafer [33] dichromatic reflection model, starting from specular-free image techniques [30, 34, 35]. These methods are based on the idea of initially generating a pseudo-diffuse component image. This provides a partial separation of the specular component,

which is later used to complete the reflection component separation of the original image. The pseudo-diffuse component image is called Specular-Free Image because it is essentially a specularly invariant representation of the input image. We tried also, remaining in the field of single-images and di-chromatic reflection model techniques, PDE-based which iteratively erodes the specular channel in the SUV color space [28], error analysis of chromaticity and appropriate selection of body color for each pixel [35], bilateral filtering [36], and intensity ratio [37] methods. Figure 5 shows some of results obtained using these techniques. We experimented both default parameters and different values to better fit our case study. We could see that the results were completely unsatisfying.

A more general approach is introduced in [38] to extract automatically two layers from an image where one layer is smoother than the other. This problem arises not only in reflection removal but also in intrinsic image decomposition. Authors introduce a strategy that regularizes the gradients of the two layers such that one has a long tail distribution and the other a short tail distribution. They formulate the problem in a probabilistic framework and describe an optimization scheme to solve this regularization

Figure 5 - Results of single images techniques of specular removal, based on dichromatic reflection model. All the algorithms are tested on the original configuration of values. Images represent the diffuse component.



with only a few iterations. A challenging issue is that if the assumption that the two layers have different smoothness is violated, the methods will fail to correctly separate the layers. Figure 6 shows that this failure appears systematically in our case.

We tried to enhance the techniques based on the use of a single image introducing a preprocessing where the image is automatically segmented to better find the highlighted area. In a second step previous illustrated techniques are used to remove the specular reflections, restoring the apparent color.

We focused on color image segmentation techniques since more utilizable than gray scale image segmentation because of their capability to enhance the image analysis process thereby improving the segmentation result.

In color image segmentation, firstly choosing a proper color space is an important issue [39]. Lab and HSV are the two most frequently chosen color spaces. Following results of [40] we have chosen Lab color space.

[41] provides an excellent reference for our work describing accurately color image segmentation techniques, and giving a classification useful to correctly analyze and implement segmentation algorithm in an automatic workflow. As in the context of color imagery, segmentation is an ill-defined problem with no perfect solution, we experimented techniques from both the sides of the classification purposed by [36]:

- spatially blind methods
- spatially guided methods.

Spatially blind approaches perform segmentation in certain attribute/feature spaces. Popular segmentation techniques that fall within the notion of being spatially blind involve clustering and histogram thresholding.

Spatially approaches are guided by spatial relationships of pixels for segmentation. Their primary objective is to form pixel groupings that are compact or homogeneous from a spatial standpoint, irrespective of their relationships in specific feature spaces. The use of region and

edge information explicitly or in an integrated framework are the widely-accepted main solutions.

Between spatially blind approaches we focused on clustering based segmentation approach, appearing more suitable with our goal to automatically select and segment the highlighted areas. In its simplest form, clustering is a spatially blind technique wherein the image data is viewed as a point cloud on a one-dimensional (1-D) gray scale axis or in a 3-D color space depending on the image type. The essence of a typical clustering protocol is to analyze this gray/color intensity point cloud and to partition it, using predefined metrics/objective functions to identify meaningful pixel groupings also known as classes or clusters. Furthermore, the clustering process is done such that, when complete, the pixel data within a specific class possess, in general, a high degree of similarity while the data between classes has low affinity. In detail, we experimented the K-Means clustering, an algorithm aiming to optimize the partitioning decisions based on a user-defined initial set of clusters that is updated after each iteration. The K-Means algorithm, in particular, partitions a set of  $n$ -pixels into  $K$  clusters by minimizing an objective function. Main limitations concern selecting/initialization of number of clusters and the fact that during the space partitioning process the algorithm does not take into consideration the local connections between the data points (color components of each pixel) and its neighbors. This fact will restrict the application of clustering algorithms to complex color-textured images since the segmented output will be over-segmented. We implemented the version of the algorithm called the *'filtering algorithm'* [42], that use a  $k$ -dimensional ( $kd$ ) tree representation of the image data. The biggest advantage of this approach was that, since the  $kd$ -tree representation was formed from the original data rather than from the computed centers, it did not mandate an update in its structure for all iterations, in contrast to the conventional K-Means architecture.

Spatially guided segmentation techniques



Figure 6 - Results of technique based on layer decomposition using a single image introduced in [31].

typically employ protocols involving growing, splitting, and merging individually or in suitable combinations. We focused on watershed transformation that can be classified as a region-based segmentation approach. The main concept of this algorithm is derived from geography. The watershed lines determine boundaries which separate image regions. The watershed transform computes catchment basins and ridgelines (also known as watershed lines), where catchment basins corresponding to image regions and ridgelines relating to region boundaries. We experimented the Meyer's watershed algorithm [43] consisting of the following basic steps:

1. Add neighbors to priority queue, sorted by value
2. Choose local minima as region seeds
3. Take top priority pixel from queue
  - a. If all labeled neighbors have same label, assign to pixel
  - b. Add all non-marked neighbors
4. Repeat step 3 until finished.

Watershed segmentation possesses several advantages such as ability to provide close contours even in low contrast regions with weak boundaries, and means to serve as a stable initialization for more sophisticated segmentation mechanisms. On the cons, the output achieved by a watershed transform is often oversegmented and requires post-processing schemes involving region merging and markers (connected components branding flat regions or objects in images) to yield a more suitable out-come.

A major portion of segmentation practices can be viewed as being either spatially blind or spatially guided. However, there are several techniques that may not distinctly fall in any of these two categories but provide good results. Between these techniques we focused on methods using specialized image features as histogram of oriented gradients (HOG), local binary patterns

(LBP), maximally stable extremal region (MSER). We experimented MSER a technique proposed by [44] to find correspondences between image elements from two images with different viewpoints. MSER technique produces blobs, i.e. highly featured regions in the sense that they are stable and salient, and have multi-scale structure. MSER regions are connected areas characterized by almost uniform intensity, surrounded by contrasting background. They are constructed through a process of trying multiple thresholds. When compared to the algorithms which rely on intensity extrema, MSER is more stable because it stems from stability extrema [45]. We referred to [46] which propose a new multi-scale image segmentation approach based on MSER. The approach can segment natural images without any user intervention. It accomplishes the segmentation by collecting MSERs and then rearranging them onto the image plane in an appropriate order that would generate desired segmentation of whole image. To denoise and smooth the region boundaries, hierarchical morphological operations and an optimal sequence of them are developed.

At the end, we processed segmented images with algorithms for single image specular removal that in the original formulation not present this extra-step and tested using the whole image. Results adding image segmentation are in Figure 7. Although some improvements have been observed, however, the road ahead remains long and hard.

After these fails, we tried another strategy: the use of techniques employing multiple images. Multi-image systems exploit information contained in an image sequence of the same scene taken either from different points of view or with different light information. Such sequence contains much more information on specularities than a single image since the specular reflection varies through the images. In the case of a sequence of images taken from different points of view, scene points showing specular reflection in a view can exhibit purely

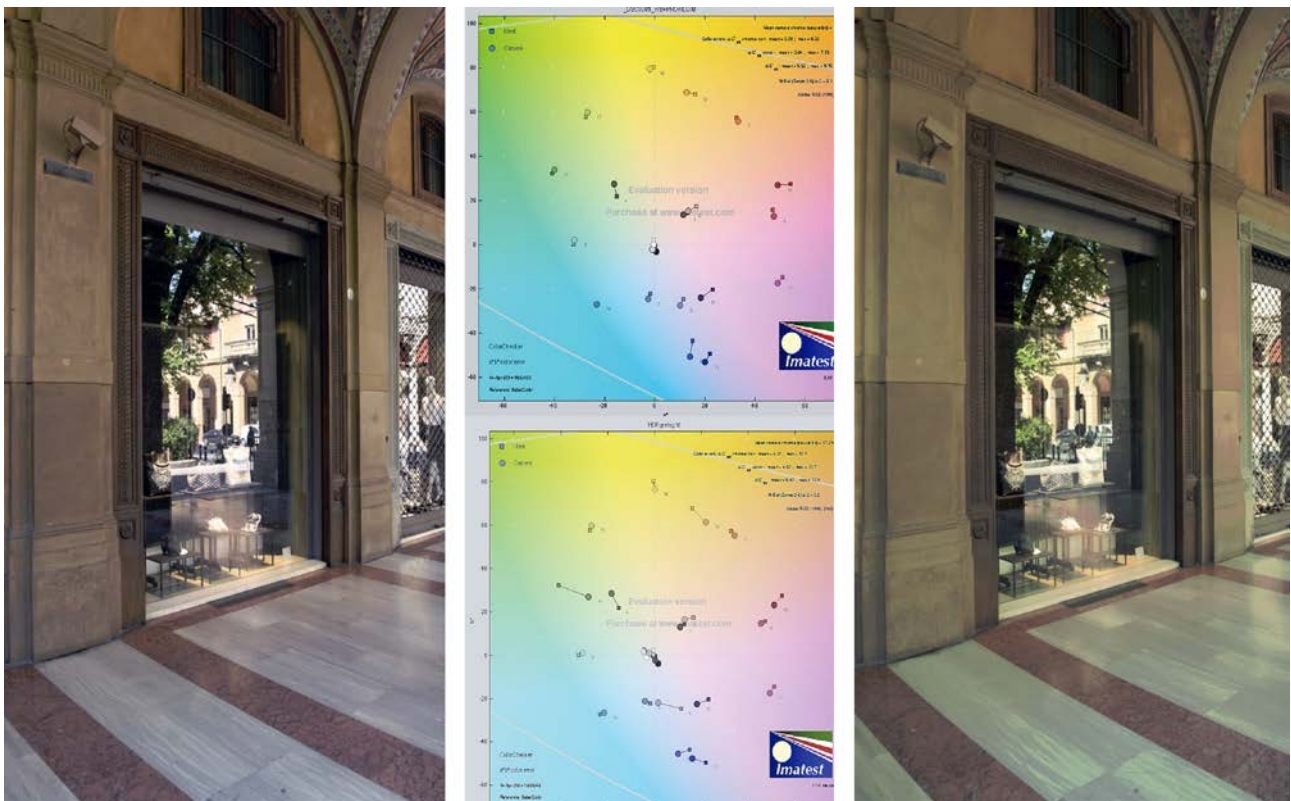
Figure 7 - Color based segmentation results on our reference image: (a) K-Means clustering technique; (b) region-based segmentation approach based on watershed transformation; (c) MSER based segmentation.



diffuse reflection in other views. By matching specular pixels to their corresponding diffuse points in other views, it is possible to determine the diffuse components of the specularities. Some methods assume a fixed camera that is able to capture a set of images with different mixing of the layers through various means, e.g. rotating a polarized lens, changing focus, applying a flash, or using HDR techniques. All these methods present many drawbacks in our context. The first three approaches demonstrate good results, but the ability of controlling focal change, polarization, and flash is rarely possible. The third technique (HDR) appear more reliable to our field, not requiring specific equipment. Some studies of last years show accurate color-calibrated tone mapped HDR images [47,48], but the algorithms in the literature were not directly usable, and their limits are still uncertain. In particular, we discarded the most recent pipeline purposed in [49] to avoid an unclear all-in-one processing. We developed a new HDR-based processing similar to that in [50]. Our goal is not only composing a single HDR from multiple color images with different exposure levels [51], but also reducing the color distortion during the tone mapping process. We capture HDR images of the scene in RAW file format, minimum camera image processing in the captured images, with and without inside a X-Rite Classic ColorChecker. The color checker is photographed under the same conditions and with the same exposure bracket as the hero shot. The calibration is performed using this single HDR image containing the X-Rite CCC,

using reference values in the CIEXYZ space [52]. We generated the HDR image using the reconstruction technique proposed from [53] following the study of the performance bounds of [54]. We tonemapped the scene image with specular reflections, trying to minimize these effects and we applied the same setting to tonemap the image with the target, using the technique proposed in [55]. Finally, we applied the same processing of color calibration applied to the other LDR images. As you can see in Figure 5, final results are not very accurate and obtained pictures are impossible to merge with the whole pipeline, where LDR images have been used. Having an HDR checker shot may not always return accurate or desirable results since the tone mapping software can sometimes create colorcasts. HDR tone mapping operators often exaggerate color-casts in a scene, and include some version of local adaptation, so the color checker is really just a starting point. To measure the error of the color corrected HDR image of ColorChecker, we calculate the average color difference  $\Delta E$  between the color-corrected HDR image and the checker reference data (Figure 5). A different approach to reflections separation consists in the exploitation of motion between multiple images [56, 57]. By analyzing the movie sequence, diffuse and specular components can be recovered. These approaches produce good results, but the constraint on scene geometry and assumed motion of the camera limit the type of scenes that can be processed. A second problem of these techniques is the indefinite number of images to be employed to

Figure 8 - On the left color calibrated LDR image, on the right color calibrated HDR image. In the middle: color difference  $\Delta E_{ab}$ ; top color calibrated LDR image, below color calibrated HDR image.



the purpose. The number of images to be used depends on working conditions, such as the distribution of ambient lighting sources and the viewing direction of the camera. Furthermore, multiple images increase both the processing time and storage. In order to reduce the number of images to be used, stereo images [58] and flash/no-flash image pairs [59, 60] have shown to provide enough information for solving the dichromatic reflection problem. Lin et al. [61] present a method based on color analysis and multi-baseline stereo that makes use of sequence of images to achieve the separation of specular reflection. Nevertheless, extra devices and equipment were incorporated. This makes very hard the practical applications of these techniques to the urban context.

A second problem in the multi-image area concerns image alignment. The use of local invariant features [2] is a powerful solution because these features are robust to typical appearance variations (illumination, blur, compression), and a wide range of 3D transformations. Initial feature matching is often followed by geometric filtering steps, which yield very reliable matches of 3D rigid scenes [62]. These operations are nothing more than the first part of our photogrammetric workflow, in this way appears easy to embed the specular removal process in the whole pipeline. Along this line [63, 64] proposed an image processing pipeline based on the use of local invariant features for building an image of a painting from a set of photographs taken with a hand-held camera in a non-controlled environment where highlights may appear. The steps of the pipeline are the following: (a) SIFT, (b) RANSAC, (c) segmentation of bursts, (d) subpixel resampling, (e) blur weighting, (f) weighted average fusion, (g) ASIFT, (h) distortion correction by polynomial approximation and subpixel resampling, (i) histogram specification, (j) vector median of gradients, and (k) Poisson fusion. To apply this workflow in our field the main drawback concerns the original assumption of like-planar surfaces and a non-simple pre-processing image alignment that limits the benefits to color fidelity without improving the results of photogrammetric pipeline.

Same problem appears with [65], where is illustrated a robust technique for layer separation from multiple images which exploits the correlation of the transmitted layer across multiple images, and the sparsity and independence of the gradient fields of the two layers. This solution need a pre-processing technique similar to [64] to accurately align images, and manual interaction to initialize the process.

Multi-image techniques and alignment using local and global features were also the last

frontier of layer separation techniques, which could be viewed as a superset of dichromatic approach. Above all these attempts to solve major lacks of the single image method [66]: the user involvement and the limited number of cases where it's possible to obtain great quality of results. The basic assumption of these algorithms is that interference decomposition should result in component images having fewer edges and corners than the original image. In [67], Levin and Weiss considered a simpler problem, in which the user provides labels of component images for a number of critical gradients in the interference image. However, the problem is still ill-conditioned. A sparsity prior was introduced, which states that the output of any derivative filter tends to be sparse. More explicitly, the histogram of the output of a derivative filter is peaked at zero and fall off rapidly out to the two extreme ends of the histogram. A probability function characterized by the sparsity prior was constructed, which served as the criterion of interference decomposition.

Features of multi-image specular removal techniques depicted their use as the most appropriate starting point for our use case.

### 3. SPECULAR REFLECTION REMOVAL METHOD

Separating reflections from a single image is an ill-posed problem, as it requires extracting two layers from one image: in absence of additional knowledge about the scene being viewed there are an infinite number of valid decompositions. To make the problem tractable additional information, either supplied from the user or from multiple images, is required.

Our approach is an improved and calibrated version of the pipeline set by [16] and [66, 67]. Moreover [66, 67] offer a solution to layer separation problem using a single image that needs to be manually labeled and where different labels represent background or reflection parts of the image itself. Following results on the statistics of natural images, these authors used a sparsity prior over derivative filters. They first approximate this sparse prior with a Laplacian prior obtaining a simple, convex optimization problem. Then they use the solution with the Laplacian prior as an initialization for a simple, iterative optimization for the sparsity prior that efficiently find the most probable decompositions using linear programming. The results show a clear advantage in a technique that is based on natural scene statistics rather than one that assume a Gaussian distribution. Beside effective results, the developed technique has a very strong constraint: it requires user intervention to label the image manually. To remove the

need for user markup, [16] suggest examining the relative motion in a small set (e.g. 3-5) of images to label gradients as either reflection or background gradients in an automatic way. First, the images are aligned using SIFT Flow [15]. Gradient variations are examined among the image set. Gradients with more variation are assumed to belong to the reflection component while constant gradients are assumed to belong to the background component. The input of [16] approach is a small set of  $k$  images of the same subject taken from slightly varying viewpoints. Authors assume that the background dominates in the mixture image and the images are related by a warping, such that the background is registered and the reflection layer is changing. This relationship can be expressed as:

$$I_i = w_i(I_{R_i} + I_B) \quad (2)$$

where  $I_i$  is the  $i$ -th mixture image,  $\{w_i\}$ ,  $i = 1, \dots, k$  are warping functions caused by the camera viewpoint change with respect to a reference image.

Pipeline steps are then, as in Figure 6:

A. For each image:

- Warping functions estimation. It is accomplished by distorting the input image to the reference image using SIFT Flow algorithm - an extension of the original SIFT Lowe technique [2] - allows extracting keypoints from an image and assigning robust descriptors to them for every image pixel. These descriptors are matched to those of another image in order to produce a list of pairs of points. This list of matching points is used to estimate the parameters of the transformation-warping vector between the two images. A robust estimation method - RANSAC - is used to automatically reject wrong matches before computing the

transformation.

- Edge separation: the presence of a static  $I_B$  in the image set allows the identification of gradient edges of the background layer  $I_B$  and edges of the changing reflection layers  $I_{R_i}$ . More specifically, edges in  $I_B$  are assumed to appear every time in the image set while the edges in the reflection layer  $I_{R_i}$  are assumed to vary across the set. This means edges can be identified evaluating the frequency of a gradient appearing at a particular pixel across the aligned input images.

- Layer Reconstruction: after labeling edges as background or reflection, the two layers are reconstructed using an optimization technique that imposes a sparsity prior on the separated layers as described by [66, 67].

B. Single images results combination. As in the original paper, we assume that the minimum value across all recovered background layers may be a proper approximation of the true background. As such, the last step is to take the minimum of the pixel value of all reconstructed background images as the final recovered background, as follows:

$$I_B(\mathbf{x}) = \min_i I_{B_i}(\mathbf{x}) \quad (3)$$

We iterate the original pipeline [16] for each initial image, as all the images were containing useful information for 3D reconstruction and all of them needed to be processed in our photogrammetric general pipeline.

Our photo datasets were mainly containing pictures of porticos. This issue increases the complexity of the problem, since this kind of photos is characterized by very high contrasts, backlight, overexposed areas and underexposed

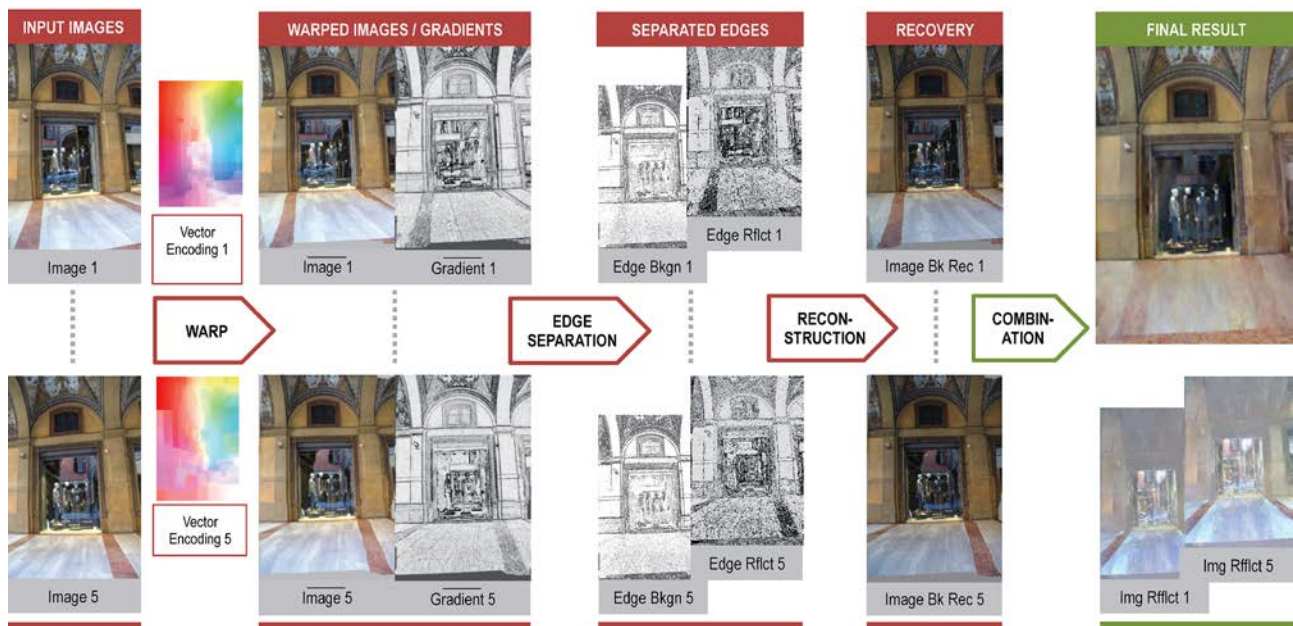


Figure 9 - Layer separation pipeline.

ones (see Figure 3). This problem has been addressed working on the separation thresholds with which gradients are identified as belonging to the background or the reflection layers.

#### 4. DISCUSSION AND RESULTS

In Figures 10, 11, 12 are the results of the use of our method to the different case of shop window and polished floor. From the point of view of the use inside the whole photogrammetric pipeline, the use of reconstructed layer separated images, leads to a strong improvement if compared to the use of original highlighted images, and we consider the study as final. Results in Figures 13, 14 and Table 1, where are reported typical parameters addressing quality

in photogrammetric processes demonstrate our affirmation.

Moreover, even if results reconstructed images apparently show many approximations and artifacts, images are evidently good enough to be processed through the whole pipeline as the software, assigning color per vertex, tends to discard the re-remaining highlighted surfaces. Effectively, if we analyze separately the layer separation results we can see that we just begin a long road. The key problem is in the warping step, with the estimation of the warping functions,  $w^{-1}_j$ , to register the input to the reference image. For our purposes, we use a combination of SIFT Flow and RANSAC to register a pair of images by a homography. This solution computes descriptors densely (i.e.

Figure 10 - Example of separation of background  $I_B$  and reflection  $I_R$  layers separation results: shop windows.



for every pixel), instead of sparsely, to have an improved registration. However, the planarity constraint often leads to reconstruct image regions slightly misaligned, especially when the scene presents elements on different planes, that is very often our case. Traditional dense correspondence method like optical flow, that are based on image intensity, even with our assumption that the background should be more prominent than the reflection layer, gave poor performance due to the reflection interference. However, images with very strong reflectance can produce poor alignment as SIFT Flow may attempt to align to the foreground, which is changing. This will cause problems in the subsequent layer separation. While these failures can often be handled by cropping the

image or simple user input, it is a notable issue. A second issue concern large displacement between images, moreover usual in our case as our sequence of images are from a photo camera and from well-spaced viewpoints. Optical flow techniques are closely related to motion estimation and motion compensation from sequence of frames and were developed for video se-quences where displacements between frames are usually limited. A basic assumption is then the local smoothness assumption. It is usually incorporated into a joint energy based regularization that rates data consistency together with the smoothness in a variational setting of the flow. One major drawback of this setting is that fast minimization techniques usually rely on local linearization of

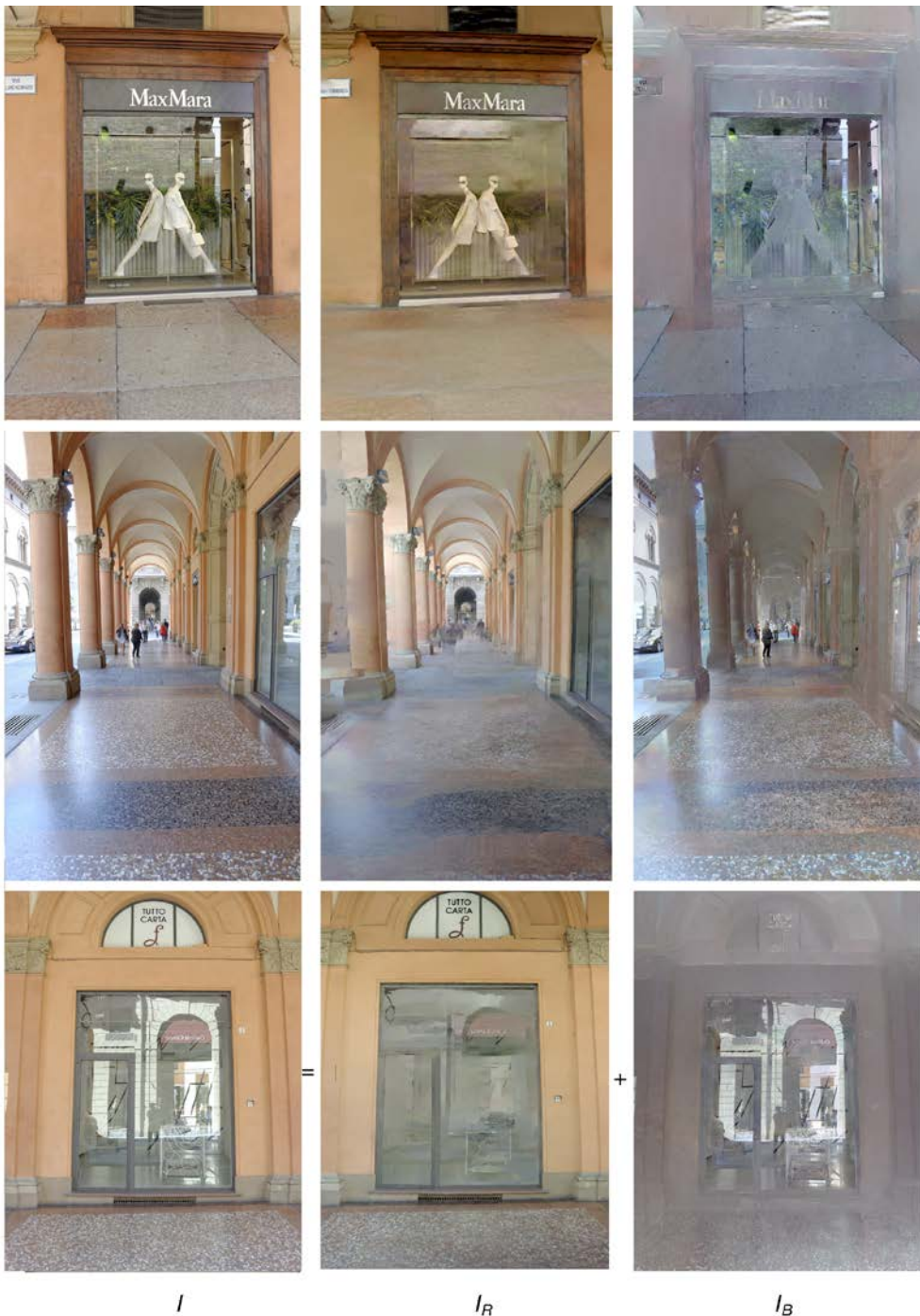


Figure 11 - Example of separation of background  $I_B$  and reflection  $I_R$  layers separation results: shop windows & porticoes.

the data term and thus can adapt the motion field only very locally. Hence, these methods have to use image pyramids to deal with large displacements [68]. In practice, this fails in cases where the determined motion on a lower scale is not very close to the correct motion of a higher scale. Also, the use of purely data based techniques like approximate nearest neighbor fields [69] (ANNF) and sparse descriptor matches [70] allow an efficient global search for the best match on the full image resolution. However, sparsity causes local gaps in the motion field that must be filled. Another challenging issue is when the background scene has large homogeneous

regions. In such cases there are no edges to be labeled as background. This makes subsequent separation challenging, especially when the reflection interference is weak but still visually noticeable.

Finally, a problem that emerges when applying dense descriptors is invariance [67]; unlike interest points, which allow for some estimation of local scale and orientation, on arbitrary image locations scale estimation is not obvious. This is a significant issue in our context, because generally images have not a clear foreground and background, and building edges sometime are oblique in respect to the picture plane. For this reason, in the future we will investigate

Figure 12 - Example of separation of background  $I_B$  and reflection  $I_R$  layers separation results: marble pavements.



Figure 13 - Final 3D model of our automatic photogrammetric pipeline. Above: using the highlighted images; below: using the layer separated images.



further scale problem.

To address these problems, we experimented some recent techniques appearing the most reliable between the many solutions developed in the last years.

To face typical invariance and background/foreground problems, we implemented a generalized image matching algorithm called DAISY Filter Flow (DFF) [71]. Following the same spirit of the SIFT Flow authors developed an algorithm achieving much more robust performance in efficiently matching images of challenging non-rigid photometric and geometric variations, or across different scenes than the existing techniques. Our approach is built upon a few established techniques but also extends them, which are 1) DAISY descriptors [72], 2)

filter-based efficient flow field inference, and 3) the PatchMatch fast search [73]. Inspired by the PatchMatch Filter (PMF) work [73], it generalizes the PMF method in two important ways: DAISY descriptors are employed and extended for general image matching; to search across scales and rotations beyond just translations. As a result, DFF algorithm allows performing spatially regularized, dense descriptor-based correspondence field estimation efficiently in a high-dimensional space. Being able to do so explains the key advantages of the DFF method in both matching robustness and computational efficiency. Results are in Figure 15.

A second attempt was made addressing the treatment of scale-invariance. We implemented Scalemap [74], a very recent algorithm aiming

	Without specular removal	With specular removal
Oriented images	<b>63/67</b>	<b>64/67</b>
PBA quality	0.130	0.087
Points from more than 3 cameras	101751	<b>114618</b>
Dense point cloud	12112000	<b>14107000</b>
Point on image_DSC3201	<b>14888</b>	2202
Inlier matches 01_02	<b>7227</b>	7435
Time matching (sec)	62	<b>1</b>

Table 1 - Photogrammetric results for the porticoes dataset



Figure 14 - Final 3D model of our automatic photogrammetric pipeline. Above: using the highlighted images; below: using the layer separated images.



Figure 15 - Separation of background  $I_B$  and reflection  $I_R$  layers separation results using [72] instead of SIFT Flow in our solution: shop window of figure 10.

to deal with the large-scale differences in different image locations. Authors demonstrated that scales estimated in sparse interest points may be propagated to neighboring pixels where this information cannot be reliably determined. In detail, they presented and implemented three different means for propagating this information: using only the scales at detected interest points (geometric propagation), using the underlying image information to guide the propagation of this information across each image, separately (image-aware propagation); and using both images simultaneously (match-aware propagation). Each of these methods considers progressively more information in order to more reliably propagate scales. We tested this approach and results are in Figure 16.

Finally, we tested Edge-Preserving Interpolation of Correspondences (EpicFlow), a novel state-of-the-art optical flow estimation method particularly suitable to approach large displacement of objects in subsequent images [75].

EpicFlow computes a dense correspondence field by performing a sparse-to-dense interpolation from an initial sparse set of matches, leveraging contour cues using an edge-aware geodesic distance. The approach builds upon the assumption that contours often coincide with

motion discontinuities and then it is easy to handle occlusions and motion boundaries. The resulting dense correspondence field is fed as an initial optical flow estimate to a one-level variational energy minimization initialized with the dense matches. Results are in Figure 17. Comparing Figures 10, 15, 16, 17 we could summarize that tested approach achieves similar performance as the SIFT Flow method in our case with slight improvements relative to the specific issue addressed. These results show that substantial improvements are possible in the future essentially trying to combine the individual effects in a global solution.

A last remark is related to the computational complexity of the method. Currently, the main problem concerns image warping that is a very expensive process, both time and memory consuming, often needing half hour and more than 128 Gb of RAM to compute our 14 Mpx images. We estimated that increasing parallelization should heavily affect time and computational resources yet maintaining consistency with the whole photogrammetric pipeline.

Figure 16 - Separation of background  $I_B$  and reflection  $I_R$  layers separation results using [75] instead of SIFT Flow in our solution: shop window of figure 10.

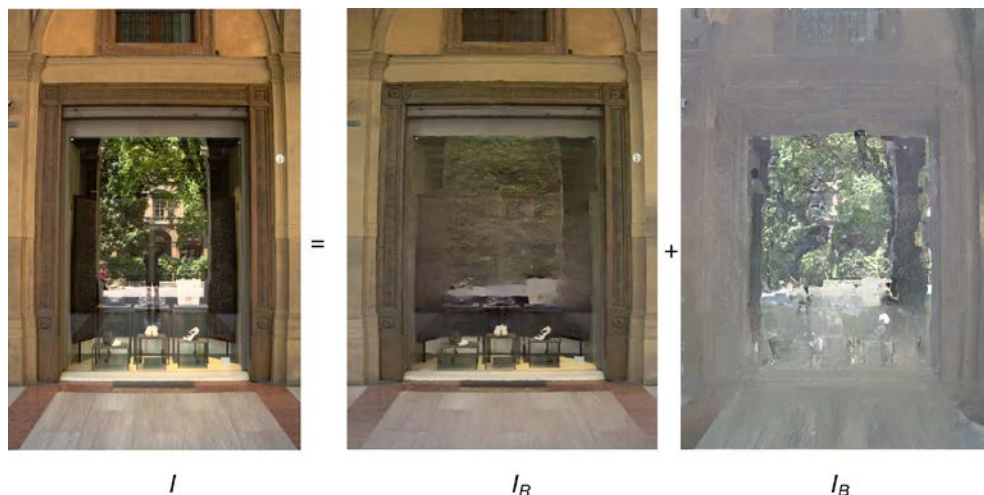


Figure 17 - Separation of background  $I_B$  and reflection  $I_R$  layers separation results using [75] instead of SIFT Flow in our solution: shop window of figure 10.



## 5. CONCLUSIONS

In this paper, we faced the problem of specular reflections, an inevitable effect in AH urban environment, in the context of automatic photogrammetry of AH 3D reconstruction and architectural modeling.

After careful evaluation of existing solutions and their applicability to our case study, we modeled the problem as layers separation problem, developing a solution completely integrated in the automatic photogrammetric pipeline. We reuse existing data to arrange new results using a multi-image technique, obtained improving and calibrating the pipeline set by [16] and [66, 67]. We iterate the original pipeline [16] for each initial image, as all the images were containing useful information for 3D reconstruction and all of them needed to be processed in our photogrammetric general pipeline.

The process of acquisition of the images to get the finished 3D model is therefore unique and the process for acquiring and visualizing the correct perceived color is fully integrated with the process of shape reconstruction.

From the point of view of the use inside the whole photogrammetric pipeline, the use of reconstructed layer separated images, leads to a strong improvement in shape reconstruction if compared to the use of original highlighted images, because unwanted effects as those in Figure 1 completely disappears.

Conversely results concerning diffuse color reconstruction are quite limited due to imprecision of the techniques existing to estimate of the warping function.

At time the best solution possible in our case to model diffuse color is to select an image where specular effect not appears or are limited and map the color directly from it. Future works will be done in this area finding warping function more accurate.

## ACKNOWLEDGMENTS

A special thanks to Li Yu, for is valuable help and for distributing the code used.

## FUNDING

This research did not receive any specific grant from funding agencies in the public, commercial, or not-for-profit sectors.

## CONFLICT OF INTEREST

The authors declare no conflict of interest.

## BIBLIOGRAPHY

- [1] N. Snavely, S.M. Seitz, R. Szeliski, "Modeling the world from internet photo collections", *IJCV*, Vol. 80, N. 2, 2008, pp. 189-210.
- [2] D. Lowe, "Distinctive image features from scale-invariant keypoints", *IJCV*, Vol. 60, N. 2, 2004, pp. 91-110.
- [3] C. Wu, et al., "Multicore bundle adjustment", *CVPR Proceedings*, pp. 3057-3064.
- [4] Y. Furukawa, J. Ponce, "Accurate, Dense, and Robust Multi-View Stereopsis", *IEEE Transactions on PAMI*, Vol. 32, N. 8, 2010, pp. 1362-1376.
- [5] F. Remondino, et al., "Low-Cost and Open-Source Solutions for Automated Image Orientation – A Critical Overview", *Euromed 2012 Proceedings*, Springer, 2012, pp. 40-54.
- [6] P. Musialski, et al., "A Survey of Urban Reconstruction", *Computer Graphics Forum*, Vol. 32, N. 6, 2013, pp. 146-177.
- [7] F.I. Apollonio, et al., "A color digital survey of arcades in Bologna", *Colour and Colorimetry Multidisciplinary Contributions*, Vol. IXB, 2013, pp. 58-68.
- [8] H.C. Lee, D.J. Breneman, C.O. Schulte, "Modeling light reflection for computer color vision", *IEEE Transactions on PAMI*, 1990, Vol. 12, pp. 402-409.
- [9] H. Barrow, J. Tanenbaum, "Recovering intrinsic scene characteristic from images", *Proceedings of the Computer Vision System*, 1978, pp. 3-26.
- [10] R. Tan, K. Ikeuchi, "Intrinsic properties of an image with highlights", *Meeting on Image Recognition and Understanding (MIRU)*, 2004.
- [11] B. K. Horn, B.G. Schunck, "Determining optical flow", *1981 Technical Symposium East Proceedings*, 1981, pp. 319-331.
- [12] S. Baker, et al., "A database and evaluation methodology for optical flow", *IJCV*, Vol. 92, N. 1, 2011, pp. 1-31.
- [13] D. Sun, S. Roth, M.J. Black, "Secrets of optical flow estimation and their principles", *CVPR Proceedings*, 2010, pp. 2432-2439.
- [14] C. Vogel, S. Roth, K. Schindler, "An evaluation of data costs for optical flow", *GCPR proceedings 2013*, pp. 343-353.
- [15] L. Ce, J. Yuen, A. Torralba, "SIFT Flow: Dense Correspondence across Scenes and Its Applications", *IEEE Transaction on PAMI*, Vol. 33, N. 5, 2011, pp. 978-994.
- [16] L. Yu, M.S. Brown, "Exploiting Reflection Change for Automatic Reflection Removal", *IEEE ICCV Proceedings*, 2013, pp. 2432-2439.
- [17] M. Ebner, C. Herrmann, "On Determining the Color of the Illuminant Using the Dichromatic Reflection Model". In: W.G. Kropatsch, R. Sablatnig, A. Hanbury (Eds), *Pattern Recognition. DAGM 2005. Lecture Notes in Computer Science*, vol. 3663. Berlin, Heidelberg: Springer, 2005.
- [18] A. Artusi, F. Banterle, D. Chetverikov, "A Survey of Specularity Removal Methods", *Computer Graphics Forum*, Vol. 30, N. 8, 2011, pp. 2208-2230.

- [19] T. Chen, et al., "Mesostructure from specularity", CVPR Proceedings, 2006, pp. 1825-1832.
- [20] B. Lamond, P. Peers, P. Debevec, "Fast image-based separation of diffuse and specular reflections", ACM SIGGRAPH 2007 sketches, ACM, New York, 2007, art. 74.
- [21] S. Lin, et al., "Diffuse-specular separation and depth recovery from image sequences", ECCV Proceedings, 2003, pp. 210-224.
- [22] Y. Weiss, "Deriving intrinsic images from image sequences", ICCV Proceedings, 2001, Vol. 2, pp. 68-75.
- [23] W.-C. Ma, et al., "Rapid acquisition of specular and diffuse normal maps from polarized spherical gradient illumination", Proceedings of the 18th Eurographics conference on Rendering Techniques, 2007, pp. 183-194.
- [24] A. Agrawal, et al., "Removing Photography Artifacts Using Gradient Projection and Flash-Exposure Sampling," ACM Trans. on Graphics, Vol. 24, N. 3, 2005, pp. 828-835.
- [25] G.J. Klinker, et al., "The measurement of highlights in color images", IJCV, 1988, Vol. 2, N. 1, pp 7-32.
- [26] K. Schluns, A. Koschan, "Global and local highlight analysis in color images", CGIP '2000 Proceedings, 2000, pp. 300-304.
- [27] H.L. Shen, Q.Y. Cai, "Simple and efficient method for specularity removal in an image", Applied Optics, Vol. 48, N. 14, 2009, pp. 2711-2719.
- [28] S.P. Mallick, et al., "Specularity removal in images and videos: A PDE approach", ECCV Proceedings, 2006, pp. 550-563.
- [29] M.F. Tappen, et al., "Recovering intrinsic images from a single image", Pattern Analysis and Machine Intelligence, IEEE Transactions on PAMI, 2005, Vol. 27, N. 9, pp. 1459-1472.
- [30] R. Tan, K. Ikeuchi, "Separating reflection components of textured surfaces using a single image", IEEE Transaction on PAMI, Vol. 27, N. 2, 2005, pp. 178-193.
- [31] E. Angelopoulou, "Specular highlight detection based on the Fresnel reflection coefficient", ICCV proceedings, 2007, pp 1-8.
- [32] L. Fang, T. Jiandong, T. Yandong, W. Yan, "An Image Highlights Removal Method with Polarization Principle", ICCMITA 2015 Proceedings, 2015, pp. 402-407.
- [33] S.A. Shafer, "Using color to separate reflection components", Color Research and Applications, Vol. 10, N. 4, 1985, pp. 210-218.
- [34] K.J. Yoon, Y. Choi, I.S. Kweon, "Fast separation of reflection components using a specularity-invariant image representation", ICIP Proceedings, 2006, pp. 973-976.
- [35] H-L. Shen, et al., "Chromaticity-based separation of reflection components in a single im-age", Pattern Recogn. Vol. 41, N. 8, 2008, pp. 2461-2469.
- [36] Q. Yang, S. Wang, N. Ahuja, "Real-time specular highlight removal using bilateral filtering", ECCV Proceedings, 2010, pp. 87-100.
- [37] H.L. Shen, Z.H. Zheng, "Real-time highlight removal using intensity ratio", Applied Optics, Vol. 52, N.19, 2013, pp. 4483-4493.
- [38] L. Yu, M.S. Brown, "Single Image Layer Separation Using Relative Smoothness", CVPR Proceedings, 2014., pp. 2752-2759.
- [39] A. Jurio, et al., "A Comparison Study of Different Color Spaces in Clustering Based Image Segmentation", Information Processing and Management of Uncertainty in Knowledge-Based Systems. Applications, Vol. 81, pp. 532-541.
- [40] D.J. Bora, A.K. Gupta, F.A. Khan, "Comparing the Performance of L\*A\*B\* and HSV Color Spaces with Respect to Color Image Segmentation", International Journal of Emerging Technology and Advanced Engineering, Vol. 5, N. 2, 2015, pp. 192-203.
- [41] S. R. Vantaram, E. Saber, "Survey of contemporary trends in color image segmentation", J. Electron. Imaging, Vol. 21, N. 4, 2012, pp. 040901-1-28.
- [42] T. Kanungo et al., "An efficient k-means clustering algorithm: analysis and implementation", IEEE Transaction on PAMI, Vol. 24, N. 7, 2002, pp. 881-892.
- [43] F. Meyer, "Topographic distance and watershed lines", Signal Processing, Vol. 38, 1994, pp. 113-125.
- [44] J. Matas, et al., "Robust wide baseline stereo from maximally stable extremal regions", BMVC Proceedings, 2002, pp. 384-396.
- [45] K. Mikolajczyk, et al., "A comparison of affine region detectors", IJCV, Vol. 65, N. 1/2, 2005, pp. 43-72.
- [46] Il-Seok Oh, Jinseon Lee, Aditi Majumder, Multi-scale Image Segmentation Using MSER, Computer Analysis of Images and Patterns Lecture Notes in Computer Science, Vol. 8048, pp. 201-208.
- [47] H.J. Yoo, et al., "Color correction of high dynamic range images at HDR-level", ACM SIGGRAPH 2007 posters, Article 67.
- [48] T-R. Chou; S.-K. Chang, "Color Calibration of Recovering HDR Images", Computer Science and Software Engineering, 2008 International Conference on, Vol. 6, 2008, pp. 286-289.
- [49] E. Reinhard, et al., "Calibrated Image Appearance Reproduction", ACM Transactions on Graphics, Vol. 31, N. 6, 2012, art. 201, 11 pp.
- [50] D. Varghese, R. Wanat, R.K. Mantiuk, "Colorimetric calibration of high dynamic range images with a ColorChecker chart", HDRi 2014, 2014, Article 4.
- [51] T. Mitsunaga, S. Nayar, "Radiometric self calibration", CVPR Proceedings, 1999, pp. 374-380.
- [52] D. Pascale, "RGB coordinates of the Macbeth ColorChecker", 2006.
- [53] M. Granados, et al., "Optimal HDR reconstruction with linear digital cameras", CVPR Proceedings, 2013, pp. 215-222.
- [54] C. Aguerrebere, et al., "Best Algorithms for HDR Image Generation. A Study of Performance Bounds", SIAM Journal on Imaging Sciences, Vol. 7, N. 1, 2014, pp. 1-34.
- [55] R. Mantiuk, S. Daly, L. Kerofsky, "Display adaptive tone mapping", ACM SIGGRAPH 2008 Proceedings, 2008, art. 68, 10 pp.

- [56] R. Szeliski, S. Avidan, P. Anandan, "Layer extraction from multiple images containing reflections and transparency", IEEE Conference on CVPR Proceedings, 2000, pp. 246-253.
- [57] M. Irani, S. Peleg, "Image sequence enhancement using multiple motions analysis", CVPR Proceedings, 1992, pp. 216-221.
- [58] Y. Tsin, S.B. Kang, R. Szeliski, "Stereo matching with reflections and translucency", CVPR Proceedings, 2003, pp. 702-709.
- [59] R. Feris, et al., "Specular reflection reduction with multi-flash imaging", SIBGRAPI04 Proceedings, 2004, Vol. 42, pp. 316-321.
- [60] A. Agrawal, et al., "Removing Photography Artifacts Using Gradient Projection and Flash-Exposure Sampling," ACM Trans. on Graphics, Vol. 24, N. 3, 2005, pp. 828-835.
- [61] S. Lin, et al., "Diffuse-specular separation and depth recovery from image sequences", ECCV Proceedings, 2003, pp. 210-224.
- [62] N. Snavely, S.M. Seitz, R. Szeliski, "Photo tourism: exploring photo collections in 3D", ACM transactions on graphics (TOG), Vol. 25, N. 3, 2006, pp. 835-846.
- [63] G. Haro, A. Buades, J.M. Morel, "Photographing paintings by image fusion", SIAM Journal on Imaging Sciences, Vol. 5, N. 3, 2012, pp. 1055-1087.
- [64] A. Buades, G. Haro, E. Meinhardt-Llopis, "Obtaining High Quality Photographs of Paintings by Image Fusion", Image Processing On Line, Vol. 5, 2015, pp. 159-175.
- [65] X. Guo, X. Cao, Y. Ma, "Robust Separation of Reflection from Multiple Images", CVPR proceedings, 2014, pp. 2195-2202.
- [66] A. Levin, A. Zomet, Y. Weiss, "Separating Reflections from a Single Image Using Local Features," CVPR Proceedings, 2004, Vol. 1, pp. 306-313.
- [67] A. Levin, Y. Weiss, "User assisted separation of reflections from a single image using a sparsity prior", IEEE Transactions on PAMI, Vol. 29, N. 9, 2007, pp. 1647-1654.
- [68] T. Brox, et al., "High accuracy optical flow estimation based on a theory for warping", ECCV proceedings, 2004, pp. 25-36.
- [69] K. He, J. Sun, "Computing nearest-neighbor fields via propagation-assisted kd-trees", CVPR proceedings, 2012, pp. 111-118.
- [70] P. Weinzaepfel, et al., "DeepFlow: Large displacement optical flow with deep matching", ICCV proceedings, 2013, pp. 1385-1392.
- [71] H. Yang, W.-Y. Lin, J. Lu, "DAISY Filter Flow: A Generalized Discrete Approach to Dense Correspondences", CVPR proceedings, 2014, pp. 3406-3413.
- [72] E. Tola, V. Lepetit, P. Fua, "DAISY: An efficient dense descriptor applied to wide-baseline stereo", IEEE Transaction on PAMI, Vol. 32, N. 5, 2010, pp. 815-830.
- [73] J. Lu, et al., "Patchmatch filter: Efficient edge-aware filtering meets randomized search for fast correspondence field estimation", CVPR proceedings, 2013, pp. 1854-1861.
- [74] M. Tau, T. Hassner, "Dense Correspondences across Scenes and Scales", IEEE Transaction on PAMI, accepted.
- [75] J. Revaud, et al., "EpicFlow: Edge-preserving interpolation of correspondences for optical flow", CVPR proceedings, 2015, pp.1164-1172.